Published by Institute of Physics Publishing for SISSA/ISAS
Received: *June 20, 2002*
Accepted: *December 9, 2002*

Turbulent diffusion and drift in galactic magnetic fields and the explanation of the knee in the cosmic ray spectrum

Julián Candia
Departamento de Física, Universidad Nacional de La Plata, CC67
La Plata 1900, Argentina
E-mail: candia@venus.fisica.unlp.edu.ar

Esteban Roulet
CONICET, Centro Atómico Bariloche
Av. Bustillo 9500, Bariloche 8400, Argentina
E-mail: roulet@cab.cnea.gov.ar

Luis N. Epele
Departamento de Física, Universidad Nacional de La Plata, CC67
La Plata 1900, Argentina
E-mail: epele@venus.fisica.unlp.edu.ar

Abstract: We reconsider the scenario in which the knee in the cosmic ray spectrum is explained as due to a change in the escape mechanism of cosmic rays from the galaxy from one dominated by transverse diffusion to one dominated by drifts. We solve the diffusion equations adopting realistic galactic field models and using diffusion coefficients appropriate for strong turbulence (with a Kolmogorov spectrum of fluctuations) and consistent with the assumed magnetic fields. We show that properly taking into account these effects leads to a natural explanation of the knee in the spectrum, and a transition towards a heavier composition above the knee is predicted.

Keywords: Integrable Equations in Physics, High Energy Cosmic Rays.

Contents

1. Introduction **1**

2. The diffusion of cosmic rays in the Galaxy **2**
- 2.1 Regular and random galactic magnetic fields 2
- 2.2 The diffusion equation 4
- 2.3 Calculation of transverse and Hall diffusion coefficients 5

3. Results and comparison with observations **8**

1. Introduction

A well established feature of the full cosmic ray (CR) energy spectrum is that it has a power-law behavior with a steepening taking place at the so-called knee, corresponding to an energy $E_{\rm knee} \simeq 3\times 10^{15}$ eV. Although the knee of the CR spectrum has been known since more than four decades, none of the numerous models proposed so far to explain this feature has managed to become broadly accepted. Some proposals focus on a possible crossover between different acceleration mechanisms below and above the knee [1]–[3], or exploit the possibility of a change in the particle acceleration efficiency [4]–[6]. Other hypotheses include the nuclear photodisintegration at the sources [7, 8], the recent explosion of a single source [9], and leakage from the Galaxy due to a change in the confinement efficiency of CRs by galactic magnetic fields [10]–[12]. Among the latter, Ptuskin et al. [12] in particular consider the knee as due to a crossover from a diffusive regime dominated by transverse diffusion at low energies to another dominated by drifts, i.e. by the Hall (antisymmetric) diffusion, above the knee. Since the diffusion coefficients determine the residence time of the CRs inside the Galaxy, this means that the observed slope of the CR energy spectrum will differ from the slope of the original average source spectrum just due to the energy dependence of the diffusion coefficients. Hence, the scenario just mentioned naturally accounts for a change in the spectral slope, arising from the diverse energy dependence of the two different diffusion coefficients.

The drift effects of CRs due to the antisymmetric diffusion depend strongly on the large scale configuration of the regular fields in the Galaxy, and in particular on the field gradients. In ref. [12] some important simplifying assumptions had to be done to make the differential equations determining the CR densities more tractable. In particular, a simplistic spatial dependence of the regular field and of the diffusion coefficients was adopted, but it was however found that the spectral slope beyond the knee was quite sensitive to the magnetic field configuration adopted and to the spatial distribution of the sources. Also, the expressions for the diffusion coefficients used were actually only valid in the limit of small turbulence. Anyhow, a feature similar to the knee was obtained, but to reproduce the correct value of $E_{\rm knee}$ a magnetic field spectrum flatter than Kolmogorov was needed.

This last requirement resulted from the fact that the perpendicular diffusion coefficient (the only one relevant for the determination of the CR densities below the knee) was normalized at low energies (few GeV) to the average value resulting from a comparison with the results of a simplified leaky box model of the Galaxy, and was then extrapolated up to $E_{\rm knee}$ using the fact that its energy dependence is directly related to the spectral index of the random magnetic fields.

In the present work we want to further elaborate on the proposal of ref. [12], but using more realistic configurations for the galactic magnetic fields (including e.g. field reversals, which enhance field gradients and can hence affect the CR drifts). We also consider diffusion coefficients appropriate for strongly turbulent magnetic fields, since strong turbulence from disturbances in the interstellar plasma is thought to be the actual picture of magnetic fields in the Galaxy, and we will directly adopt diffusion coefficients normalized from the results of numerical simulations valid in the relevant energy range of the knee and consistent with the magnetic fields adopted.

The beauty of this scenario is that in it the presence of a break in the spectrum does not require any special assumption, but just follows from properly taking into account well established properties of the propagation of charged particles in regular and turbulent magnetic fields. Moreover, this break naturally happens at the energies at which the knee is actually observed.

2. The diffusion of cosmic rays in the Galaxy

2.1 Regular and random galactic magnetic fields

The Milky Way, as well as other spiral galaxies, is known to have a large-scale regular magnetic field $\mathbf{B_0}(\mathbf{x})$, which is determined by measurements of the rotation due to the Faraday effect of the polarization plane of radiation from pulsars and extra-galactic radio sources [13, 14]. The magnetic lines are observed to follow the spiral arms, but there is a variety of models to describe the regular magnetic field structures. Models of magnetic fields of spiral galaxies are distinguished between bisymmetric (BSS) and axisymmetric (ASS), defined so that BSS (ASS) fields are antisymmetric (symmetric) with respect to a π rotation. For a spiral galaxy with two arms, for instance, in BSS models the field reverses its sign between the arms, while in ASS models it keeps the same orientation. In the case of the Milky Way, the regular magnetic field in the galactic disk is predominantly toroidal, being aligned with the spiral structure and having reversals in direction between nearby arms. Hence, the regular field in the disk is usually described with a BSS model. Furthermore, magnetic field models can be classified as symmetric (S) or antisymmetric (A) with respect to the galactic plane, and the regular disk component is believed to be symmetric with respect to the galactic plane. The presence of substantial non-thermal radio emission at high galactic latitudes points to the existence of an extended corona with non-negligible magnetic fields. This magnetic halo extends possibly up to 10 kpc from the galactic plane. Although the orientation of the regular field in the galactic halo is not known, the toroidal component appears to be dominant. The magnetic field structure of the halo may be similar to that of the galactic disk (for instance if its origin is related to a galactic wind which somehow extends the field disk properties into the halo), but it may also be different since it could be independently generated through a dynamo mechanism.

Taking into account the main features of the regular magnetic field in the Galaxy mentioned above, we will assume that the propagation region of the galactic CRs is a cylinder of radius $R = 20\,\mathrm{kpc}$ and height $2H$, with a halo size $H = 10\,\mathrm{kpc}$. Moreover, since the pitch angle of the spiral arms is quite small ($< 10^\circ$), it is a good approximation to consider that the regular magnetic field is directed in the azimuthal direction. We will hence adopt cylindrical coordinates (r, ϕ, z) throughout, taking $\mathbf{B_0} = B_0\hat{\phi}$ and assuming for simplicity that the system has azimuthal symmetry. In passing, notice that a $\phi-$independent azimuthal field is necessarily divergenceless. In order to reproduce the field reversals of the BSS-S model, we will adopt for the regular disk component the expression

$$B_0^{\rm disk}(r,z) = B_d \frac{1}{\sqrt{1+(r/r_c)^2}}\frac{1}{\sqrt{1+(z/z_d)^2}} \sin\left(\frac{\pi r}{4\ \rm kpc}\right) {\rm th}^2\left(\frac{r}{1\ \rm kpc}\right), \qquad (2.1)$$

where $r_c = 4\,\mathrm{kpc}$ is a core radius which smoothes out near the galactic center the overall $1/r$ behavior, $z_d = 1\,\mathrm{kpc}$ is the adopted magnetic disk scale height, and the value of B_d is chosen such that $B_0^{\rm disk}(r_{obs}, z_{obs}) = -2\ \mu\mathrm{G}$ at our observation point ($r_{obs} = 8.5\,\mathrm{kpc}$, $z_{obs} = 0$).[1] Notice the minus sign arising from the fact that the local galactic magnetic field is nearly directed towards the longitude $l \simeq 90^\circ$, i.e. in the $-\hat{\phi}$ direction. This regular field component has reversals for $r = 4$, 8, 12 and 16 kpc. For the regular halo component, we will consider it to be described either by a field structure with radial reversals, namely

$$B_0^{\rm halo}(r,z) = B_h \frac{1}{\sqrt{1+(r/r_c)^2}}\frac{1}{\sqrt{1+(z/z_h)^2}} \sin\left(\frac{\pi r}{4\ \rm kpc}\right) {\rm th}^2\left(\frac{r}{1\ \rm kpc}\right), \qquad (2.2)$$

or by a model without radial reversals, as given by

$$B_0^{\rm halo}(r,z) = B_h \frac{1}{\sqrt{1+(r/r_c)^2}}\frac{1}{\sqrt{1+(z/z_h)^2}} {\rm th}^2\left(\frac{r}{1\ \rm kpc}\right) \mathcal{R}, \qquad (2.3)$$

where $z_h = 5\,\mathrm{kpc}$ is the adopted magnetic halo scale height, and B_h is such that $B_0^{\rm halo}(r_{\rm obs}, z_{\rm obs}) = \pm 1\,\mu\mathrm{G}$. The function $\mathcal{R}$ is just unity for the symmetric halo case, and it is taken as $\mathcal{R}(z) = {\rm sign}(z)$ in the case of a halo model antisymmetric with respect to the galactic plane.

Eqs. (2.1)–(2.3) provide simple but yet realistic galactic magnetic field models, containing the characteristic features (such as the reversals) which we believe are important for the determination of the drift effects.

Superimposed to the regular magnetic field structures of the galactic disk and the extended halo, an irregular magnetic field $\mathbf{B_r}(\mathbf{x})$ due to turbulence in the interstellar plasma is known to exist, with the largest eddies having a scale $L_{\rm max} \simeq 100\,\mathrm{pc}$. This random field component has a strength comparable to the field of the regular component, namely

[1] The ${\rm th}^2(r)$ factor multiplying the regular magnetic field components just insures that there are no singularities in the $r = 0$ axis, something which would otherwise artificially introduce a singular drift current along that axis (see below).

$\langle|\mathbf{B_r}|\rangle/\langle|\mathbf{B_0}|\rangle \sim 1$–3 locally. The existing observational data [15] show that the spectrum of inhomogeneities may be the same for the density of the gas and for the magnetic field, and that it is close to a Kolmogorov spectrum. Hence, the random magnetic field can be assumed to be given by a power-law spectrum with Fourier components giving rise to a magnetic energy density $\mathrm{d}E/\mathrm{d}k \propto k^{-5/3}$, for $k \geq 2\pi/L_{\rm max}$. The random field intensity will be considered to possess a smooth spatial dependence analogous to the envelope of the regular fields assumed above, namely

$$|\mathbf{B_r}(r,z)| = B_r^* \frac{1}{\sqrt{1+(r/r_c)^2}} \frac{1}{\sqrt{1+(z/z_r)^2}}\,, \tag{2.4}$$

where $z_r = 3$–$5\,\mathrm{kpc}$ and B_r^* is such that $|\mathbf{B_r}(r_{\rm obs}, z_{\rm obs})| = 2$–$4\,\mu\mathrm{G}$. Since we are concerned with highly relativistic particles of speed $v \simeq c$, which is much larger than the Alfvén velocity v_A characteristic of the magnetic wave propagation, it is well justified to assume the magnetic disturbances to be static, and thus to neglect electric fields.

2.2 The diffusion equation

On scales larger than the scale of magnetic irregularities, the cosmic ray transport across the turbulent galactic magnetic fields can be well described by means of a diffusion equation, in which the components of the diffusion tensor depend on both the regular field and the random turbulence. Neglecting nuclear fragmentation and any energy losses, the steady-state diffusion equation for the cosmic ray density $N(\mathbf{x})$ reads

$$\nabla \cdot \mathbf{J} = Q(\mathbf{x})\,, \tag{2.5}$$

where Q is a source term and the CR current is given by

$$J_i = -D_{ij}(\mathbf{x})\nabla_j N(\mathbf{x})\,. \tag{2.6}$$

In general, the diffusion tensor D_{ij} can be written as

$$D_{ij} = \left(D_{\parallel} - D_{\perp}\right) b_i b_j + D_{\perp}\delta_{ij} + D_A \epsilon_{ijk} b_k\,, \tag{2.7}$$

where $\mathbf{b} = \mathbf{B_0}/|\mathbf{B_0}|$ is a unit vector along the regular magnetic field, δ_{ij} is the Kronecker delta symbol, and ϵ_{ijk} is the Levi-Civita fully antisymmetric tensor. The symmetric terms contain the diffusion coefficients parallel and perpendicular to the mean field, $D_{\parallel}$ and $D_{\perp}$, which describe diffusion due to small-scale turbulent fluctuations. The antisymmetric term contains the Hall diffusion coefficient D_A, which is responsible for the particle drifts. The diffusion equation can be rewritten as

$$-\nabla_i D_{Sij} \nabla_j N + u_i \nabla_i N = Q\,, \tag{2.8}$$

where $D_{Sij} = (D_{\parallel} - D_{\perp}) b_i b_j + D_{\perp}\delta_{ij}$ contains the symmetric part of the diffusion tensor, and $u_i = -\epsilon_{ijk}\nabla_k (D_A b_j)$ is called the drift velocity. Notice also that the CR current in eq. (2.6) may be written as

$$\mathbf{J} = -D_{\perp}\nabla_{\perp} N - D_{\parallel}\nabla_{\parallel} N + D_A \mathbf{b} \times \nabla N\,, \tag{2.9}$$

JHEP12(2002)033

where $\nabla_{\|} \equiv \mathbf{b}(\mathbf{b}\cdot\nabla)$ and $\nabla_{\perp} \equiv \nabla - \nabla_{\|}$. Hence, the macroscopic drift current is orthogonal to the overall direction of the regular field and to the CR density gradient.

Under the assumption mentioned previously that the regular magnetic field is directed in the azimuthal direction (i.e. $b_r = b_z = 0$, with $b_\phi = \pm 1$), and that the system has azimuthal symmetry ($\partial/\partial\phi = 0$), eq. (2.5) simplifies to

$$\left[-\frac{1}{r}\frac{\partial}{\partial r}\left(rD_{\perp}\frac{\partial}{\partial r}\right) - \frac{\partial}{\partial z}\left(D_{\perp}\frac{\partial}{\partial z}\right) + u_r\frac{\partial}{\partial r} + u_z\frac{\partial}{\partial z}\right] N(r,z) = Q(r,z)\,, \tag{2.10}$$

where the drift velocities are

$$u_r = -\frac{\partial(D_A b_\phi)}{\partial z} \tag{2.11}$$

and

$$u_z = \frac{1}{r}\frac{\partial(rD_A b_\phi)}{\partial r}\,. \tag{2.12}$$

These expressions for the drift velocities already make apparent the possible relevance of including field reversals in the regular fields, since this certainly affects the spatial gradients of the diffusion coefficients.

At the surface Σ corresponding to the boundaries of the halo, the CR density has to become negligible, since particles can escape freely into the intergalactic space. The boundary conditions that apply to eq. (2.10) are thus $N|_\Sigma = 0$.

Notice that the diffusion treatment of the CR propagation will be adequate as long as the Larmor radius, which for a relativistic particle of energy E and charge Z is given by

$$r_L \equiv \frac{pc}{Ze|\mathbf{B_0}|} \simeq \frac{E/Z}{10^{15}\,\mathrm{eV}}\left(\frac{|\mathbf{B_0}|}{\mu\mathrm{G}}\right)^{-1}\mathrm{pc}\,, \tag{2.13}$$

is smaller than the typical scale height of the magnetic field. Hence, for CRs trapped in the disk of the Galaxy, this requires $E/Z <$ few $\times\, 10^{17}$ eV, and somewhat larger values could result if the magnetic fields in the halo were sizeable. Clearly the knee region is well inside this domain.

2.3 Calculation of transverse and Hall diffusion coefficients

The components of the diffusion tensor that define the CR diffusion process through eqs. (2.10)–(2.12) depend on both the regular field and the random turbulence, but unfortunately a comprehensive theory capable of determining the diffusion coefficients from our knowledge about the magnetic fields is lacking.

From quite general considerations concerning the ensemble average of the two-time particle velocity correlations, i.e. $R_{ij}(t) \equiv \langle v_i(t_0)v_j(t_0+t)\rangle$, applied to the Taylor-Green-Kubo formula [16], the following theoretical relations involving the diffusion coefficients are expected to hold:

$$D_{\|} = \frac{vr_L}{3}\omega\tau_{\|}\,, \tag{2.14}$$

$$D_{\perp} = \frac{vr_L}{3}\frac{\omega\tau_{\perp}}{1+(\omega\tau_{\perp})^2}\,, \tag{2.15}$$

and

$$D_A = \frac{v r_L}{3} \frac{(\omega \tau_A)^2}{1 + (\omega \tau_A)^2} , \tag{2.16}$$

where $v \simeq c$ is the particle speed and $\omega \equiv v/r_L$ is the angular gyrofrequency.[2] It should be noticed that three different timescales $\tau_{||}, \tau_\perp$ and τ_A appear here as the effective timescales for the decorrelation of particle trajectories. Indeed, the trajectory decorrelation due to a given component of the diffusion tensor will be in general associated to some particular physical processes which may not always be contributing to the other components of the diffusion tensor. For instance, for low turbulence levels the field line random walk appears as the dominant contribution to the transverse diffusion, but it plays no major role in the parallel diffusion.

There is however no general theory providing the decorrelation timescales. In particular, this turns out to be a severe restriction for the study of particle diffusion under highly turbulent conditions. It should be noticed that in treating CR diffusion in the Galaxy we are precisely concerned with high turbulence levels, not only because the mean random magnetic field is of the order of the mean regular field, but also because when there are reversals in the orientation of the regular field, there exist regions in which the regular field becomes negligible and hence inside them the turbulence largely prevails.

To go beyond the general expressions in eqs. (2.14)–(2.16) requires then to make some simplifying assumptions about the timescales for decorrelations. For instance, in ref. [16] a common decorrelation timescale τ was assumed to hold for both the perpendicular and the antisymmetric diffusion ($\tau \equiv \tau_\perp = \tau_A$). It was then assumed that the major contribution to perpendicular diffusion is due to field line random walk and, based on simple considerations, the Ansatz

$$\omega \tau = \frac{2}{3} \frac{r_L}{D_{\rm flrw}} , \tag{2.17}$$

was adopted to relate the decorrelation timescale to the diffusion coefficient $D_{\rm flrw}$ associated with the field line random walk. Provided either an analytical or numerical estimate for $D_{\rm flrw}$, which depends on both the form of the turbulence spectrum and the turbulence level assumed, $D_\perp$ and D_A are thus obtained. However, the numerical study of ref. [17] shows that the Ansatz proposed in [16] leads to results clearly inconsistent with the simulations, so it may be concluded that eq. (2.17) is not appropriate to model all effects contributing to the randomization of the particle trajectories.

Expressions similar to eqs. (2.14)–(2.16), but in which only a single timescale τ appears for the three diffusion coefficients, were obtained in several previous analytic studies that assumed a single scattering process to be responsible for all the decorrelations. This happens, for instance, by considering a nearly isotropic particle distribution under an homogeneous scattering process, in which τ represents the characteristic time of isotropization [18]. A similar structure was also found for collisional diffusion coefficients in a plasma in thermal equilibrium [19]. Furthermore, regarding τ as the scattering time, these expressions can also

[2] The sign of D_A in eq. (2.16) corresponds to the diffusion of positively charged particles, and the opposite sign will hold for negatively charged ones.

JHEP12(2002)033

be obtained by treating the magnetic disturbances as hard-sphere scattering centers [20], and is known as the "classical scattering result" [21]–[23].

Very recently, Casse et al. [24] presented extensive Monte Carlo measurements of parallel and transverse diffusion of relativistic test particles propagating in strong stochastic Kolmogorov fields, extending previous numerical results [17]. From these investigations, it turns clearly out that the extrapolation of the previously mentioned theoretical models to account for particle diffusion in strongly turbulent fields is generally not applicable. For instance, the numerical simulations [17, 24] show that, while eq. (2.14) for parallel diffusion appears to agree well with the obtained results, eq. (2.15) for transverse diffusion (with $\tau \equiv \tau_{||} = \tau_{\perp}$) clearly fails, as expected from the fact that field line random walk is in general not negligible.

Given these facts, what we will do instead is to directly extract the transverse diffusion coefficient from the numerical results of ref. [24]. These results will be applicable in the regime of interest for the study of the knee region, since the relevant energy parameter, $\rho \equiv 2\pi r_L/L_{\max}$, takes the value $\rho \simeq 0.1$ for protons near the knee, which is just inside the range [0.001,10] explored in ref. [24].

In ref. [24] $D_{\perp}$ was obtained as a function of rigidity and turbulence level (their figure 5), were the turbulence level is defined as $\eta \equiv B_r^2/(B_r^2 + B_0^2)$. It turns out that an approximate expression for $D_{\perp}$, valid in the range $0.1 \leq \eta \leq 1$, is just

$$D_{\perp} \simeq 8.7 \times 10^{27} e^{3.24\eta} \left(\frac{\bar{r}_L}{\mathrm{pc}}\right)^{1/3} \frac{\mathrm{cm}^2}{\mathrm{s}} , \tag{2.18}$$

where $\bar{r}_L$ is an effective Larmor radius defined as in eq. (2.13) but replacing $|\mathbf{B_0}| \to \sqrt{B_0^2 + B_r^2}$. It should be remarked that, although this expression is obtained from numerical simulations, the dependence on rigidity through a power 1/3 appears also in theoretical expressions (valid in the limit of small turbulence) under the assumption of a Kolmogorov spectrum for the random fields [12].

Regarding the drift effects, there are at present no numerical studies concerning the Hall diffusion under turbulent conditions, so that some additional assumptions had to be made. Notice first that from eq. (2.16) we can obtain the value of D_A in the two limiting cases of very strong or weak turbulence. In the first case, i.e. for $\omega\tau_A \to 0$, one has as expected that $D_A \to 0$, so that drift effects become small (this limit is of particular interest in the regions with field reversals, in which the turbulence will tend to suppress the drift effects). On the other hand, in the limit of very weak turbulence ($\omega\tau_A \gg 1$), the obtained expression tends to the well-known result $D_A = vr_L/3$ of the quasi-linear approximation. In order to obtain a smooth transition between the two limiting regimes, and lacking theoretical or numerical results for τ_A, we will just adopt eq. (2.16) for D_A but assuming here a common timescale for all decorrelation processes. Under the assumption of a common decorrelation timescale, it turns out in particular that

$$\frac{D_{||}}{D_{\perp}} = 1 + (\omega\tau)^2 , \tag{2.19}$$

and this ratio was obtained as a function of rigidity and turbulence level in ref. [24] (see their figure 6). The ratio $D_{||}/D_{\perp}$ turns out to be almost independent of the energy in the range studied, and using eq. (2.19) we find that the simple approximate relation $\omega\tau \simeq 4.5(|\mathbf{B_0}|/|\mathbf{B_r}|)^{1.5}$ reasonably reproduces the numerical results for $D_{||}/D_{\perp}$. This result for $\omega\tau$ may now be replaced in eq. (2.16) (after changing $\tau_A \to \tau$) and this provides an expression for the Hall diffusion coefficient. The resulting expression for D_A has the proper behavior in the limits of very strong or very weak turbulence, and the criterium adopted to obtain $\omega\tau$ just allows to get a smooth transition between the two regimes. We do not expect the general results obtained to change qualitatively if a different prescription to regulate D_A were adopted. Anyhow, further investigations concerning the Hall diffusion under turbulent conditions are currently under progress.

3. Results and comparison with observations

We have assumed the regular galactic magnetic field to be composed of a disk component with radial reversals and symmetric with respect to the galactic plane (given by eq. (2.1)), and a halo component which could be described either by a field structure with radial reversals (eq. (2.2)) or by a model without radial reversals (eq. (2.3)). In the former case, it is supposed that the halo is an extension of the disk magnetic field, and hence it will be considered to be also symmetric with respect to the galactic plane and directed parallel to the disk component throughout the Galaxy. In contrast, in the latter case all relevant variants concerning symmetry and orientation will be explored, since this case may correspond to an independently generated halo field. Hence, in this case four different configurations arise from choosing the orientation (through the sign of B_h) and the symmetry with respect to the galactic plane (through the function $\mathcal{R}$).

Adopting a certain galactic field model and assuming a given source distribution $Q(r,z)$, the CR diffusion is determined by solving the diffusion equation given by eqs. (2.10)–(2.12). Following ref. [12], the sources are assumed to lie on a thin disk of height $2h_s = 400\,\mathrm{pc}$, so that the source term takes the form $Q(r,z) = q(r)\theta(h_s - |z|)$, where θ is the Heaviside function. Concerning the radial source distributions, both localized[3] (i.e., $q(r) \propto \delta(r - r_s)$, with $r_s = 3$ and $6\,\mathrm{kpc}$) and extended ($q(r) = \mathrm{const.}$) distributions have been studied. The resulting differential equation has been solved numerically using the Crank-Nicolson discretization and the Liebmann method [25].

In order to illustrate the role of drifts in the CR diffusion, let us first consider a localized source at $r_s = 6\,\mathrm{kpc}$, and adopting for the random field an amplitude $|\mathbf{B_r}(r_{\mathrm{obs}}, z_{\mathrm{obs}})| = 2\,\mu\mathrm{G}$ and a scale height $z_r = 3\,\mathrm{kpc}$. Figures 1(a) and (b) show the spatial distribution of the CR density within the Galaxy, assuming a halo without radial reversals and symmetric with respect to the galactic plane, for energies both below and above the knee. As expected from the preceding discussions, it is observed that at low energies the CR particle diffusion is mainly due to small-scale turbulent fluctuations (governed by $D_{\perp}$), while at higher energies the bulk of the CRs is driven according to the drifts that arise from the large-scale regular magnetic field, leading to significant large-scale asymmetries in the CR density distribution.

[3] These sources actually correspond to rings around the galactic center, since a non-central point-like source would break the azimuthal symmetry assumed.

JHEP12(2002)033

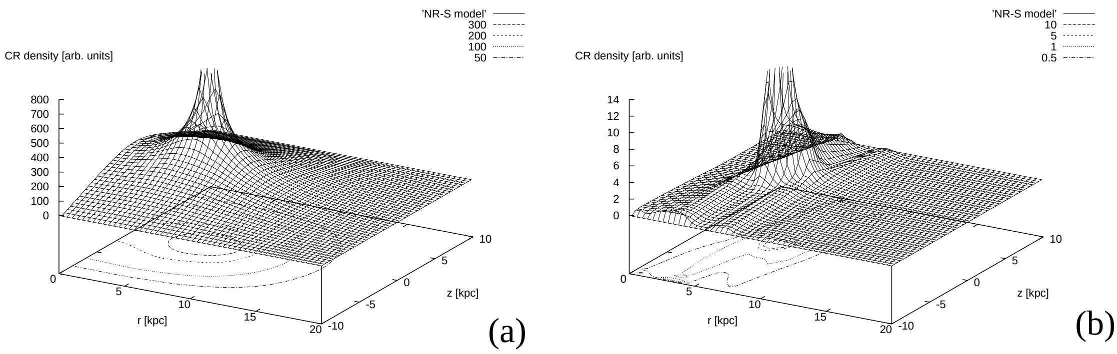

Figure 1: Spatial distributions of the CR density within the Galaxy, assuming a halo without radial reversals and symmetric with respect to the galactic plane, for a source localized at $r_s = 6\,\mathrm{kpc}$. Notice that the sharp peaks occurring around the source location have been truncated. (a) At low energies below the knee the CR particle diffusion is mainly due to small-scale turbulent fluctuations (governed by $D_\perp$). (b) At high energies above the knee, drifts arising from the large-scale regular magnetic field lead to significant large-scale asymmetries in the CR density distribution.

The influence of the drift effects on the CR spectrum at our observation point depends on the galactic field model, on the particular set of parameters considered within the given model (i.e. the field amplitudes and scale heights assumed for both the regular and random field components), and on the source distribution. Notice that the relevant parameter in the diffusion coefficient is the Larmor radius of the CRs, implying that the impact of drift effects will depend on the CR rigidity, and hence on the value of E/Z.

Figure 2 shows the normalized CR flux ϕ as a function of E/Z for the different regular galactic field models described in section 2.1 with the same source and local random field amplitude as in figure 1. The random field scale height considered is $z_r = 5\,\mathrm{kpc}$. Notice that in this and the following figures, the CR flux appears multiplied by $E^{\gamma_Z+1/3}$, where γ_Z is the spectral index corresponding to the component of charge Z at the source (see eq. (3.1) below). Since transverse diffusion depends on rigidity through a power 1/3 (see eq. (2.18)), it turns out that $\phi E^{\gamma_Z+1/3}$ is flat at low energies well below the knee. $R-S$ denotes the halo with radial reversals and symmetric with respect to the galactic plane, while $NR-S(A)$ refers to the halo without radial reversals and symmetric (antisymmetric) with respect to this plane. Furthermore, the orientation of the halo relative to the regular disk component is distinguished by means of the sign of $B_d \cdot B_h$.

It can be seen that most of the models considered show the appropriate tendency to account for the knee, since a steepening in the spectrum appears at the right value of E/Z (i.e. for $E \simeq E_{\mathrm{knee}}$ for protons, and higher for heavier nuclei). Drift effects are particularly enhanced for the antisymmetric halo case, as could be anticipated from eq. (2.11) since for $b_\phi \simeq \pm\mathrm{sign}(z)$ one has $u_r \simeq \mp 2D_A\delta(z)$ on the galactic plane, and this additional contribution to the drifts significantly affects the results. Moreover, the halo contribution to the vertical drift velocity u_z will be converging (or diverging) from both sides of the galactic plane (rather than being similarly oriented as in the symmetric models). One

JHEP12(2002)033

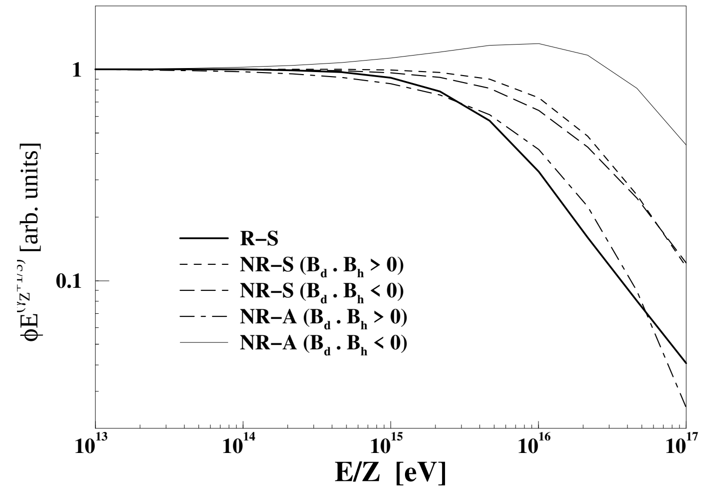

Figure 2: Plots of the normalized differential energy spectrum versus E/Z for the different regular galactic field models investigated. $R-S$ denotes the halo with radial reversals and symmetric with respect to the galactic plane, while $NR-S(A)$ refers to the halo without radial reversals and symmetric (antisymmetric) with respect to this plane. Furthermore, the orientation of the halo relative to the regular disk component is distinguished by means of the sign of $B_d \cdot B_h$, as indicated.

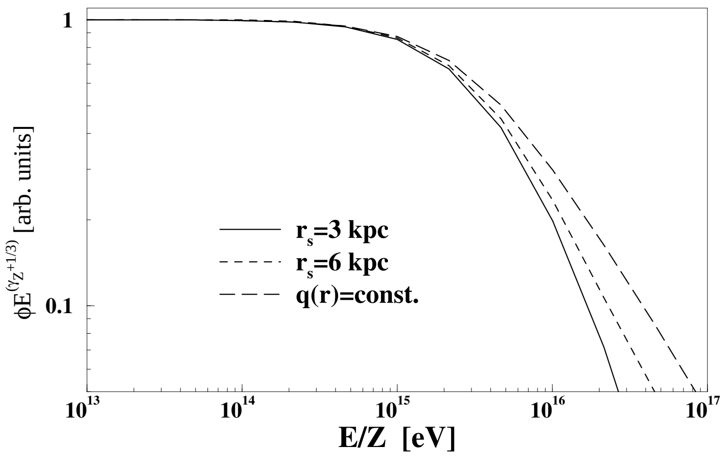

Figure 3: Plots of the normalized differential energy spectrum versus E/Z for the $R-S$ case and different source distributions, namely homogeneously extended ($q(r)$ = const.) and localized sources ($q(r) \propto \delta(r - r_s)$, with $r_s = 3$ and $6\,\mathrm{kpc}$).

obtains in this case a more pronounced knee for $B_d \cdot B_h > 0$, while a flattening of the spectrum just before the knee is observed for $B_d \cdot B_h < 0$. The pronounced bump observed in figure 2 for this case is in disagreement with the observed spectra, so that this model would be observationally disfavored. However, the possible existence of a smaller bump just below the knee in the actual data was noticed by Kempa et al. [26] many years ago, although it still remains somewhat controversial. It is interesting however that features of this kind may arise from drift effects in some particular configurations of regular galactic magnetic fields.

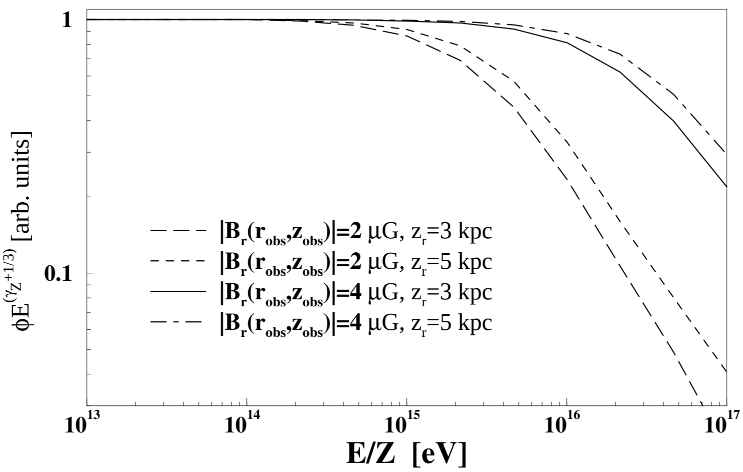

Figure 4: Plots of the normalized differential energy spectrum versus E/Z for the $R-S$ case and a source localized at $r_s = 6\,\text{kpc}$. The random field parameters take the values $|\mathbf{B_r}(r_{\text{obs}}, z_{\text{obs}})| = 2$ or $4\,\mu\text{G}$ and $z_r = 3$ or $5\,\text{kpc}$, as indicated.

Figure 3 shows the $R-S$ case for an extended source distribution $q(r) = \text{const.}$, as well as for sources localized at $r_s = 3\,\text{kpc}$ and $r_s = 6\,\text{kpc}$, with the same random field as in figure 1. As may be expected, the drift effects appear stronger the farther the source is located, since drift effects can remove high energy CRs from the galactic plane all the way from the source to the observer. The same qualitative behavior has also been observed in the other cases studied.

Figure 4 displays the effects of varying the parameters relevant to the random field. The data correspond to the $R-S$ case and the random field parameters take the values $|\mathbf{B_r}(r_{\text{obs}}, z_{\text{obs}})| = 2$ or $4\,\mu\text{G}$ and $z_r = 3$ or $5\,\text{kpc}$. As expected, the drifts are clearly stronger when the random field is suppressed, either by decreasing its overall amplitude or its scale length. Again, the same qualitative behavior has been observed in the other relevant field configurations, and is due to the increased suppression of D_A under stronger turbulence conditions.

To compare our results with experimental data, it is assumed that the differential fluxes of different nuclei emitted by the sources have power-law distributions, i.e.

$$\phi_Z^0(E) = \Phi_Z^0 E^{-\gamma_Z}\,, \tag{3.1}$$

where $1 \le Z \le 26$. The intensities Φ_Z^0 and spectral indices γ_Z were taken from the detailed knowledge about CR mass composition below the knee (and for energies per particle above $\sim few\ \ Z \times 10^{10}\,\text{eV}$) [27], and they were then extrapolated to energies above the knee. Making the convolution of the spectrum of each component of charge Z with the modulation effects produced by the drifts discussed previously and summing over all components from hydrogen to iron, we arrive at the all-particle CR flux given by the model, which can then be compared with the observed spectra measured by different experiments (KASCADE, CASABLANCA, DICE, PROTON satellite, and Akeno) [28]–[32].

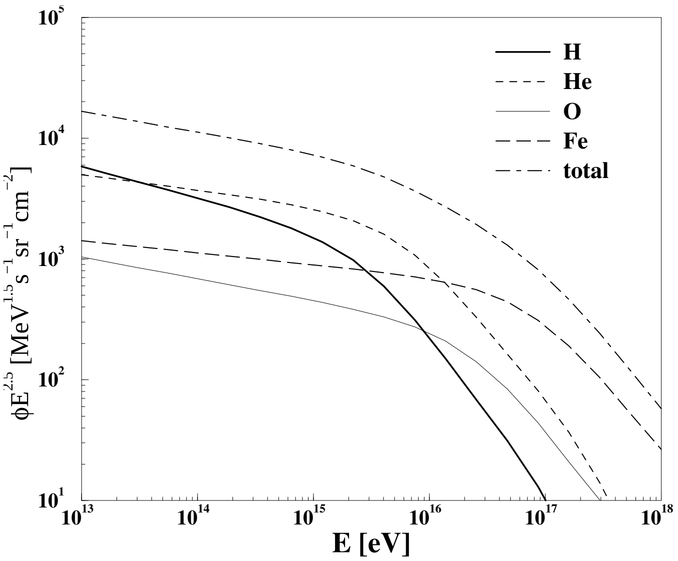

Figure 5: Plots showing the main contributions to the total CR flux coming from protons and nuclei of helium, oxygen and iron, calculated in the $R-S$ case for a source localized at $r_s = 6$ kpc.

Figure 5 shows the main contributions to the total CR flux coming from protons and nuclei of helium, oxygen and iron, calculated in the $R-S$ case for a source localized at $r_s = 6$ kpc, with the random field parameters as in figure 1. Figure 6(a) shows the total CR flux corresponding to this case compared with some observations, and clearly a very satisfactory agreement is found between the predictions and the actual experimental data. As discussed above and shown in preceding figures, varying model parameters and considering other galactic field models enables to obtain somewhat different spectra. We do not attempt here to make a detailed quantitative test of the different models, both because the different data still have sizeable statistic (and systematic) uncertainties, and because the predictions also rely on several simplifying assumptions. For instance, the transport equation was regarded as purely diffusive, neglecting spallation of nuclei in the interstellar medium or convection due to the possible existence of a galactic wind. Also, the spatial dependence of the various components of the magnetic field in the Galaxy were taken as smooth as possible in order to simplify the integration of the differential equations determining the CR densities. Although the adopted models are plausible and capture the main expected features of the galactic magnetic fields, certainly the real ones will be less idealized. Moreover, a (sensible) prescription for dealing with the Hall diffusion under turbulent conditions had to be adopted, due to the lack of appropriate numerical studies concerning this issue at present. Hence, an accurate fit to the experimental data is not to be expected, although it is reassuring to observe that the predictions within this scenario tend to exhibit a remarkable agreement with observations.

Figure 6(b) shows a plot of the mean mass composition $\langle \ln A \rangle$ versus E corresponding to the same case as before. For comparison, we also show the CR mass composition measured by different experiments [28]–[32]. Since leakage from the Galaxy depends on E/Z and is more effective for lighter particles, this scenario can easily account for a change

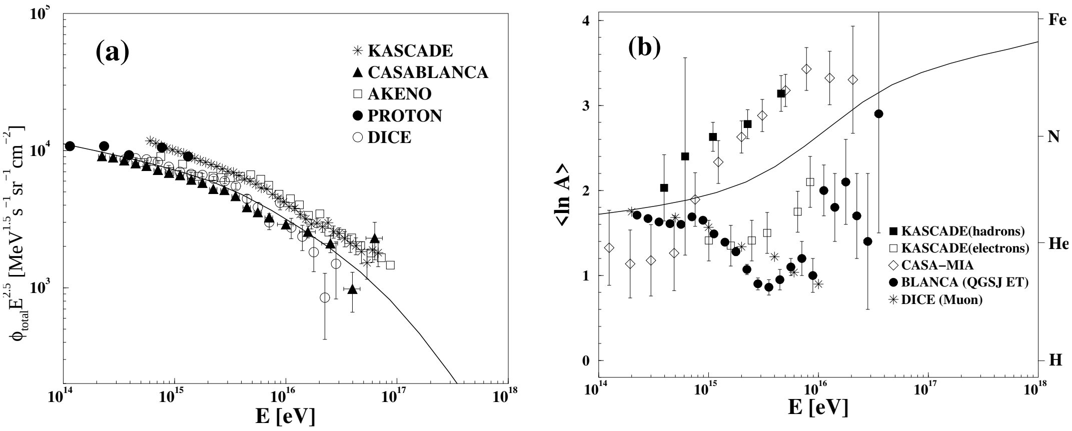

Figure 6: Comparison between experimental observations and model predictions obtained in the $R - S$ case for a source localized at $r_s = 6\,\mathrm{kpc}$: (a) plot of the total CR flux versus the energy per particle; (b) plot of the mean mass composition $\langle \mathrm{lnA} \rangle$ versus the energy per particle.

in the composition towards heavier nuclei above the knee, which is apparent on some of the existing data and in particular in the latest KASCADE observations [32]. However, since above 10^{14} eV nucleus the information about the CR mass composition has to be obtained indirectly from extensive air shower observations at ground level, still significant discrepancies are found between the results of experiments using different techniques. Indeed, the CR mass composition beyond the knee is not definitively established yet, with some observations [28] suggesting that it could turn lighter while others finding that the heavier components become dominant [31, 32]. In figure 6(b) it can be seen that some data sets suggest that the mean mass composition has a dip starting at $E \simeq 10^{15}$ eV, while it grows steadily towards heavier components beyond $E \simeq 3 \times 10^{15}$. A dip corresponding to the composition becoming lighter could possibly result from a bump in the spectrum of the proton component in the same energy range. The models predict on the other hand that for increasing energies only the heavier elements persist, since the lighter ones are efficiently drifted away for $E/Z \gg E_{\mathrm{knee}}$.

As a summary, we have considered in detail the diffusion and drift effects of CRs in realistic configurations of the galactic magnetic fields, adopting diffusion coefficients appropriate for the high levels of turbulence present in the Galaxy and for a Kolmogorov spectrum of fluctuations. On the one hand, the larger field gradients associated to the field reversals present between spiral arms enhance the drift effects, but on the other hand a suppression of D_A associated to the high turbulence present (particularly near field reversals) tends to reduce the drifts, so that the two effects compete among each other. We used diffusion coefficients obtained directly through numerical simulations valid in the relevant energies, and found that the correct value of E_{knee} can easily be obtained. Although the slope of the spectrum of each nuclear component changes by a factor $\Delta\alpha \simeq -2/3$ from below to above ZE_{knee}, the envelope of the total spectrum shows a milder change in slope, which is consistent with the observed spectrum. A progressive transition towards a heavier composition results in this scenario.

JHEP12(2002)033

Certainly a better knowledge of the CR spectrum and especially of the CR mass composition around and above the knee is of major importance to finally decide which is the correct mechanism responsible for this feature.

Acknowledgments

Work supported by CONICET, ANPCyT and Fundación Antorchas, Argentina.

References

[1] P.O. Lagage and C.J. Cesarsky, *The maximum energy of cosmic rays accelerated by supernova shocks*, *Astron. Astrophys.* **118** (1983) 223; *Cosmic-ray shock acceleration in the presence of self-excited waves*, *Astron. Astrophys.* **125** (1983) 249.

[2] P.L. Biermann, *Cosmic rays: origin and acceleration. What we learn from radio astronomy, Inv. Rap. High. Papers* 45, 23th ICRC, Calgary, 1993.

[3] L.C. Drury et al., *The gamma-ray visibility of supernova remnants. A test of cosmic ray origin*, *Astron. Astrophys.* **287** (1994) 959.

[4] C.E. Fichtel and J. Linsley, *High-energy and ultra-high-energy cosmic rays*, *Astrophys. J.* **300** (1986) 474.

[5] J.R. Jokipii and G.E. Morfill, *Ultra-high-energy cosmic rays in a galactic wind and its termination shock*, *Astrophys. J.* **312** (1986) 170.

[6] K. Kobayakawa, Y. Sato and T. Samura, *Acceleration of particles by oblique shocks and cosmic ray spectra around the knee region*, *Phys. Rev.* **D 66** (2002) 083004 [astro-ph/0008209].

[7] S. Karakula and W. Tkaczyk, *The formation of the cosmic ray energy spectrum by a photon field*, *Astropart. Phys.* **1** (1993) 229.

[8] J. Candia, L.N. Epele, and E. Roulet, *Cosmic ray photodisintegration and the knee of the spectrum*, *Astropart. Phys.* **17** (2002) 23 [astro-ph/0011010].

[9] A.D. Erlykin and A.W. Wolfendale, *High-energy cosmic ray mass spectroscopy, 2. Masses in the range* $10^{14}\,eV$ *to* $10^{17}\,eV$, *Astropart. Phys.* **7** (1997) 203; *Astropart. Phys.* **10** (1999) 69.

[10] S.I. Syrovatsky, *Comm. Astrophys. Space Phys.* **3** (1971) 155.

[11] J. Wdowczyk and A.W. Wolfendale, *Galactic cosmic rays above* $10^{18}\,eV$, *J. Phys.* **G 10** (1984) 1453.

[12] V.S. Ptuskin et al., *Diffusion and drift of very high energy cosmic rays in galactic magnetic fields*, *Astron. Astrophys.* **268** (1993) 726.

[13] A.A. Ruzmaikin, A.M. Shukurov and D.D. Sokoloff, *Magnetic fields of galaxies*, Kluwer Academic Press, Dordrecht 1988.

[14] J.L. Han, *Magnetic fields in our galaxy: how much do we know?*, *Astrophys. Space Sci.* **278** (2001) 181 [astro-ph/0010537].

[15] J.W. Armstrong, J.M. Cordes, and B.J. Rickett, *Density power spectrum in the local interstellar medium*, *Nature* **291** (1981) 561.

[16] J.W. Bieber and W.H. Matthaeus, *Perpendicular diffusion and drift at intermediate cosmic-ray energies*, *Astrophys. J.* **485** (1997) 655.

[17] J. Giacalone and J.R. Jokipii, *The transport of cosmic rays across a turbulent magnetic field*, *Astrophys. J.* **520** (1999) 204.

[18] P.A. Isenberg and J.R. Jokipii, *Gradient and curvature drifts in magnetic fields with arbitrary spatial variation*, *Astrophys. J.* **234** (1979) 746.

[19] R. Balescu, H.-D. Wang, and J.H. Misguich, *Langevin equation versus kinetic equation: subdiffusive behavior of charged particles in a stochastic magnetic field*, *Phys. Plasmas* **1** (1994) 3826.

[20] L.J. Gleeson, *The equations describing the cosmic-ray gas in the interplanetary region*, *Planet. Space Sci.* **17** (1969) 31.

[21] E.N. Parker, *The passage of energetic charged particles through interplanetary space*, *Planet. Space Sci.* **13** (1965) 9.

[22] S. Chapman and T.G. Cowling, *The mathematical theory of non-uniform gases*, Cambridge University Press, Cambridge 1970.

[23] M.A. Forman and L.J. Gleeson, *Cosmic-ray streaming and anisotropies*, *Astroph. and Sp. Sci.* **32** (1975) 77.

[24] F. Casse, M. Lemoine and G. Pelletier, *Transport of cosmic rays in chaotic magnetic fields*, *Phys. Rev.* **D 65** (2002) 023002 [astro-ph/0109223].

[25] W.H. Press et al., *Numerical recipes*, 2nd ed., Cambridge University Press, Cambridge 1992.

[26] J. Kempa, J. Wdowczyk and A.W. Wolfendale, *The energy spectrum of primary cosmic rays above* $10^12\,eV$, *J. Phys.* **A 7** (1974) 437.

[27] B. Wiebel-Sooth and P.L. Biermann, *Cosmic rays, VII. Individual element spectra: prediction and data*, *Astron. Astrophys.* **330** (1998) 389.

[28] S.P. Swordy and D.B. Kieda, *Elemental composition of cosmic rays near the knee by multiparameter measurements of air showers*, *Astropart. Phys.* **13** (2000) 137 [astro-ph/9909381].

[29] J.W. Fowler et al., *A measurement of the cosmic ray spectrum and composition at the knee*, *Astropart. Phys.* **15** (2001) 49 [astro-ph/0003190].

[30] S.P. Swordy et al., *The composition of cosmic rays at the knee*, *Astropart. Phys.* **18** (2002) 129 [astro-ph/0202159].

[31] KASCADE collaboration, K.-H. Kampert et al., *The KASCADE air shower experiment: composition analyses and energy spectrum*, OG. 1.2.11, Proceedings of 26th ICRC, Salt Lake City, 1999.

[32] KASCADE collaboration, K.H. Kampert et al., *Cosmic rays in the energy range of the knee: recent results from kascade*, astro-ph/0102266.

JHEP12(2002)033